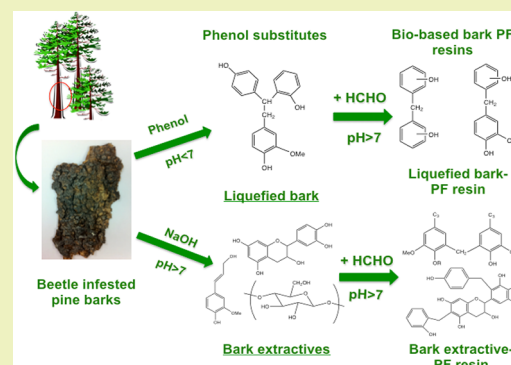


Biobased Phenol Formaldehyde Resins Derived from Beetle-Infested Pine Barks—Structure and Composition

Yong Zhao,[†] Ning Yan,^{*,†} and Martin W. Feng[‡][†]Faculty of Forestry, University of Toronto, 33 Willcocks Street, Toronto, Ontario, Canada M5S 3B3[‡]FPIInnovations—Wood Products Division, 2665 East Mall Vancouver, British Columbia, Canada V6T 1W5

ABSTRACT: In this study, two types of biobased bark-derived phenol formaldehyde (PF) resins, namely, liquefied bark-PF and bark extractive-PF, were synthesized from acid-catalyzed phenol-liquefied bark and bark alkaline extractives, respectively. The biobased resins were characterized for their chemical compositions and molecular structures using the liquid-state ¹³C nuclear magnetic resonance (NMR) technique. The results indicated that the introduction of bark components (either as liquefied bark or as bark extractives) to the phenolic resin synthesis affected resin structures and curing performance. Methylene ether bridges were found in the bark-derived PF resins. Bark components made the formation of *para-ortho*-methylene linkage more favorable in bark-derived PF resins than in lab PF resins. Molecular structures of the liquefied bark-PF resin differed significantly from those of the bark extractive-PF resins. The liquefied bark-PF resin showed a higher ratio of *para-para/ortho-para*-methylene link ($-\text{CH}_2-$), a higher unsubstituted/substituted hydrogen ($-\text{H}/-\text{CH}_2\text{OH}$) ratio and a higher methylol/methylene ($-\text{CH}_2\text{OH}/-\text{CH}_2-$) ratio than the bark extractive-PF resin. The tannin components of the bark extractives accelerated the curing rate of the resulting bark extractive-PF resin. The bark extractives made the *ortho* position of phenol react more favorably with formaldehyde than the *para* position. The liquefied bark with phenolated structures had more reactive sites toward formaldehyde than the bark extractives and accelerated the curing rate of the resulting liquefied bark-PF resin.

KEYWORDS: Bark-derived PF resins, Liquefied bark, Bark extractives, Chemical structures, Curing characteristics, Liquid-state ¹³C NMR



INTRODUCTION

Phenol formaldehyde (PF) resins, obtained through reacting phenol with formaldehyde, have been widely used as adhesives, coatings, thermal insulation materials, and molding compounds because of their good mechanical properties and heat resistance.¹ With the increasing concern on fossil fuel depletion and environmental footprint, there is a strong global interest to explore renewable resources as alternative feedstocks for making PF resins. Phenol formaldehyde resins containing tannins, lignin, bark, etc. are some of the examples.

Bark, a nonfood-related biomass material available in large quantities, is a residue from forest operations and mills. Compared with wood, bark has a similar chemical composition but contains more extractives and phenolic compounds. Bark and bark phenolic compounds have been used to partially substitute petroleum-based phenol in the resin synthesis.^{2–7} In recent studies, both phenol-liquefied bark-PF resins² and alkaline bark extractive-PF resins³ were synthesized. In those studies, lap-shear bonding strengths under the wet and dry conditions of the bark extractive-PF and liquefied bark-PF resins were compared with those of a laboratory-made control PF resin (lab PF) without bark components and a commercial oriented strand board (OSB) face layer PF resin.^{2,3} The lab PF was synthesized following exactly the same procedure for the bark-

derived PF resins. The commercial PF resin was used to give a benchmark for the bonding strength even though its formulation details were unknown. It was found that the wet bonding strength of the liquefied bark-PF resin was higher than that of the commercial PF resin while the dry bonding strength was similar. Meanwhile, the bark extractive-PF resins with 50 wt % phenol replacement by bark extractives exhibited similar dry and wet bonding strengths to those of the lab control PF (lab PF) resin without any bark component.² The curing rate of the liquefied bark-PF resin was less than that of the commercial PF resin but higher than that of the lab-made PF resin.³ The curing behavior and curing kinetics of both types of bark-derived PF resins at various phenol substitution levels differed significantly from those of the lab PF resin.^{2,3}

Liquid-state ¹³C nuclear magnetic resonance (NMR) spectroscopy has been successfully applied to characterize the composition of phenol-liquefied cellulose, phenol-liquefied cellulose and lignin model compounds, bark tannin extractives, and PF resins.^{8–28} The NMR studies on the phenol liquefaction of cellulose, cellobiose, and guaiacylglycerol- β -guaiacyl ether

Received: July 11, 2012

Revised: November 11, 2012

Published: November 16, 2012

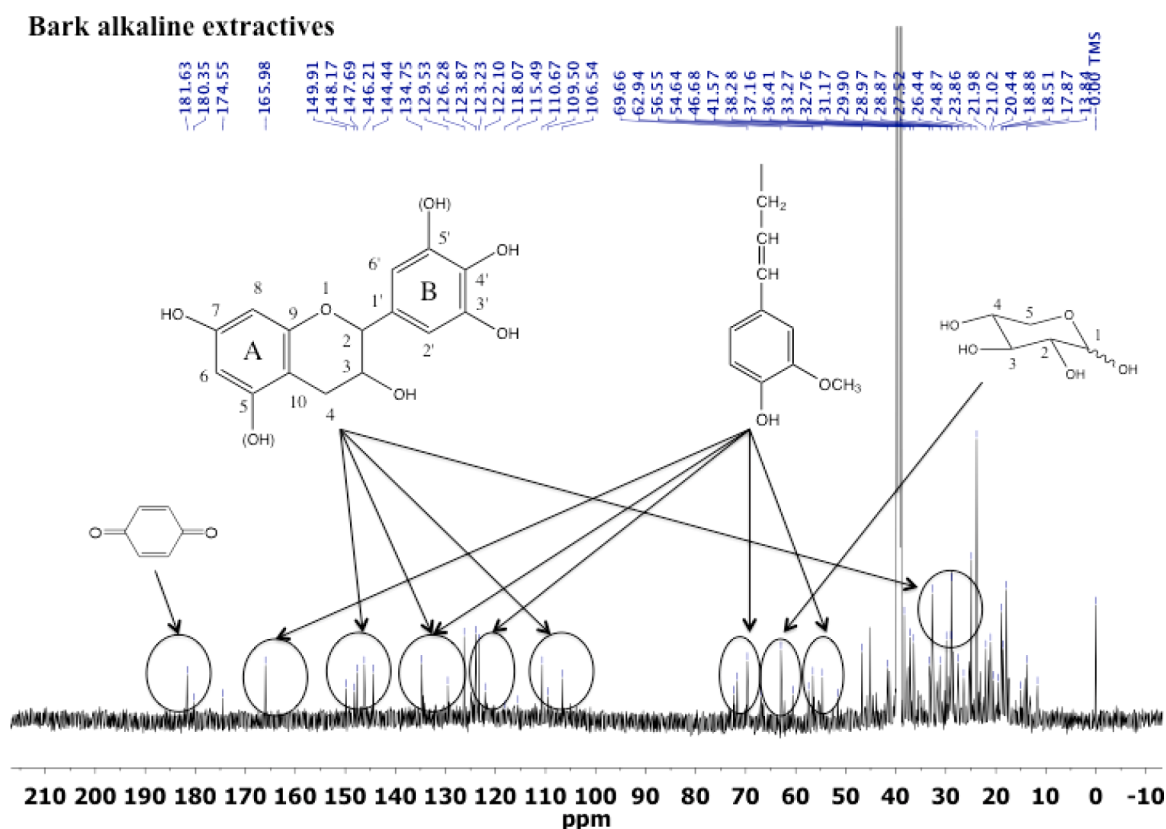


Figure 1. Liquid-state ^{13}C NMR spectrum of the bark alkaline extractives.

(GG) showed that phenol reacted with these compounds during the liquefaction.^{8–11} It was found that compounds formed during cellulose liquefaction had structural units, such as methylol phenol, that highly resembled conventional PF resins.⁸ The liquefaction of GG formed intermediates that were highly reactive and could further condense with each other or with phenol. The main liquefied products of GG, such as diphenylmethanes and guaiacol, were highly phenolated and could be used for phenolic resin synthesis.^{9,10}

NMR studies on the commercial bark tannin extractives, such as black wattle tannin extracts, mimosa tannin extracts, quebracho tannin extracts, pine tannin extracts, and bark sodium sulfite extractives from radiata pine and maritime pine have identified different structures of polyflavonoid tannins and their degrees of polymerization.^{12–16} The structure and reactivity of tannins varied significantly among tree species and extraction methods. Numerous NMR studies on the PF resins in the literature provided qualitative and quantitative information on the resins' reaction mechanisms, structures, and compositions.^{17,18} It was generally believed that methylene linkage was the dominant structure in these resins and no methylene ether linkage was reported for the uncured resol resins under the alkaline conditions.^{20,22,24,26} Methylene ether bridges between phenol rings are not stable and could be eliminated under the alkaline conditions.²⁸ In addition, ^{13}C NMR also provided useful information for investigating the cure-accelerated PF and PUF resins.^{19,20} However, scarce information on molecular structures of biobased bark-derived PF resins can be found in the literature. A better fundamental understanding of the resin compositional characteristics is needed in order for these environmentally more friendly resins to be adopted commercially.

In this study, liquid-state ^{13}C NMR was used to elucidate the compositional structures of the phenol-liquefied bark, bark alkaline extractives, and the liquefied bark-PF and bark extractive-PF resins. Moreover, the bark-derived PF resin structures identified by the liquid-state ^{13}C NMR were compared with the resin-curing properties measured by the differential scanning calorimeter (DSC) to better understand the reaction mechanism and curing behavior of these resins.

EXPERIMENTAL SECTION

Bark Liquefaction. Mountain pine beetle (MPB; *Dendroctonus ponderosae*) infested lodgepole pine (*Pinus contorta*) bark was first ground into powders that could pass through 0.500 mm size mesh screen (35-mesh) and was oven-dried at 105 °C for 12 h before liquefaction. The bark powders were then liquefied in phenol with a bark to phenol weight ratio of 1:3 using concentrated sulfuric acid (96%) as the catalyst (3% of phenol weight). The liquefaction reaction was conducted at 150 °C for 120 min. The liquefied products were diluted by methanol (150 mL) and then filtered using Millipore filter paper (Whatman). The methanol insoluble portion was removed and recorded as residues of bark liquefaction. The methanol soluble fraction containing liquefied bark was then subjected to rotary evaporation for methanol removal; the liquefied bark (about 85 wt % yield from original bark) was obtained for the subsequent liquefied bark-PF resin synthesis.

Bark Extraction. Air-dried mountain pine beetle-infested lodgepole pine bark powders (100 g oven-dry weight) that had passed through 0.500 mm sieve (35-mesh) were extracted by 500 mL of 1% NaOH aqueous solution in a boiling water bath for 2 h. Extraction was repeated two more times. Each extract was then filtered through the Whatman filter paper (110 mm Ø). The resulting alkaline filtrates from the three-stage extractions were combined together and were dried at 60 °C to constant weights. The resulting solid extractives (about 60 wt % yield from bark with a Stiasny number equal to 38%) were ground by mortar and pestle into powders for the subsequent resin synthesis.

Resin Synthesis. Liquefied bark-phenol formaldehyde (LBPF) resin and bark extractive-phenol formaldehyde (BEPF) resin were synthesized according to the methods reported previously.^{2,3} A calculated amount of liquefied bark, 37% formaldehyde, and 40% sodium hydroxide (1/3 of total NaOH weight) were mixed in a three-necked flask for liquefied bark-phenol formaldehyde formulation. Meanwhile, a calculated amount of bark extractives in powder form, phenol (crystal form), 37% formaldehyde, and 40% sodium hydroxide (1/3 of total NaOH weight) were mixed in another three-necked flask for formulating bark extractive-phenol formaldehyde resin. For both resins, the reaction temperature increased from room temperature to 65 °C within 30 min and was kept at 65 °C for 10 min in an oil bath, followed by the addition of the remaining 2/3 of 40% NaOH. The reaction mixture was then heated to 85 °C and kept at 85 °C for 60 min. After the reaction, the reactor mass was cooled down to room temperature. The laboratory-made PF resin (lab PF) without bark components was prepared by following exactly the same reaction steps used for the synthesis of the bark-derived PF resins. All the chemicals were purchased from Caledon Laboratory Chemicals, Canada, and used without further purification. A commercial liquid PF resin for the oriented strand board (OSB) face layers provided by FPInnovations was used for comparison.

Liquid-State ¹³C NMR Measurement. The liquefied bark, bark extractives, liquefied bark-PF resin, and bark extractive-PF resins were first dissolved in DMSO-*d*₆ (dimethyl sulfoxide). The liquefied bark was dissolved in DMSO-*d*₆ as liquid after removal of MeOH by rotary evaporation. Bark extractives were dissolved in the solid state after oven-drying. The liquefied bark-PF and bark extractive-PF resins were dissolved in DMSO-*d*₆ as aqueous resins with solids content of 52.97% and 47.90%, respectively. The liquefied bark, bark extractives, liquefied bark-PF resin, and bark extractive-PF resin all were soluble in DMSO-*d*₆. The liquid-state ¹³C NMR spectra of these samples were recorded using a Unity 500 spectrometer under the following conditions: a pulse angle of 60° (8.3 μs), a relaxation delay of 10 s, and with gated Waltz-16 1H decoupling during the acquisition period. About 400 scans were accumulated for each spectrum. The ¹³C chemical shifts were measured using tetramethylsilane (TMS) as the internal standard.

RESULTS AND DISCUSSION

Liquid-State ¹³C NMR Spectrum of the Bark Alkaline Extractives. The liquid-state ¹³C NMR spectrum of bark alkaline extractives is shown in Figure 1. The assignment of the chemical shifts according to previous studies is listed in Table 1.^{12,16,29–32,34–36} The chemical shifts observed in the regions around 150, 145, and 133 ppm were primarily associated with polyphenolic procyanidin and prodelphinidin tannins and lignins.¹⁶

The chemical shift at 181 ppm was attributed to the carbonyl group in the quinone structure due to the oxidation of phenolic hydroxyl groups. The chemical shift at 174 ppm belonged to either catechin or epicatechin gallate, suggesting the C=O bond of a gallic residue linked to catechin or epicatechin gallate.¹²

The tannin flavonoid structure existing in the bark alkaline extractives was shown as the chemical shift at about 150 ppm representing C5 and C7 attached to the phenolic –OH group on the flavonoid A-ring, while shifts at 140–145 ppm representing the C3' and C4' on the B-ring and shifts at 131, 116–118, 110–115, and 105 ppm indicating the C1', C5' and C2', C4–C8, and C4–C6 interflavonoid bonds, respectively. The chemical shift at 68 ppm was associated with C3 located in the chain interior and upper chain-ending positions. The chemical shift at 29 ppm was assigned to C4.³⁴ The intensity of this chemical shift was affected by the oligomeric carbohydrates in the bark extractives. The chemical shift at 36.5 ppm belonged to the C4 involved in the interflavonoid bond, whereas the chemical shift at 19.5 ppm was attributed to the free C4. These two peaks indicate the degree of polymerization of tannins in the bark extractives. It can be seen

Table 1. Assignment of Chemical Shifts for Bark Alkaline Extractives^{12,34–36}

chemical shifts (ppm)	assignment
181	C=O in quinone structures
174	catechin or epicatechin gallate
166	CH-γ in <i>p</i> -coumarate ester
150	C5, C7 on tannin phenolic A ring
140–145	C3', C4' on tannin phenolic B ring
133–135	C-1 in guaiacyl and syringyl unit
131	C1' on tannin phenolic B ring
122	C6 in the guaiacyl units
116–118	C5' on tannin phenolic B ring
110–115	C4–C8 interflavonoid bond
105	C4–C6 interflavonoid bond
72.4	CH-α in the β-O-4' (erythro) guaiacyl
71.6	CH-γ in β-β' units and CH-α in the β-O-4 (threo) guaiacyl
69.6	CH-4 in xylose nonreducing end unit
68	C3 on the tannin phenolic A ring
62.9	Cγ in the β-O-4 structures
55.6	methoxyl groups
54.6	CH-β in β-β' units
36.5	C4 interflavonoid bond
19.5	free C4 on tannin phenolic A ring

that the intensity of the chemical shift at 110–115 ppm was higher than that at 105 ppm, suggesting the tannins in the bark alkaline extractives from the mountain pine beetle infested lodgepole pine was mainly procyanidin. The intermediate intensity of the chemical shift at 116 ppm indicated the existence of the pyrogallol-type B-ring and catechol B-ring in the tannins from the alkaline pine bark extractives. The chemical shift of C1' at 130–132 ppm for the catechol B-rings and 132–135 ppm for the pyrogallol B-rings also supported the coexistence of the catechol B rings and pyrogallol B-rings in the tannins from the bark alkaline extractives.

In addition, lignin fragments in the bark extractives were also present. The chemical shift at 55.6 ppm was assigned to the methoxyl groups in the lignin. The chemical shift at 62.9 ppm corresponded to Cγ in the β-O-4 structure. The chemical shift at 122 ppm was related to the C6 in the guaiacyl units. The chemical shifts at 133–135 ppm were attributed to C1 in guaiacyl and syringyl units. The chemical shifts at 72.4 and 71.6 ppm were assigned to CH-α in the β-O-4' (erythro) guaiacyl, CH-γ in β-β' units, and CH-α in the β-O-4 (threo) guaiacyl, respectively. The chemical shift at 54.6 ppm was CH-β in β-β' units. Hemicellulose structures could also be seen in the bark extractives. The chemical shift at 69.6 ppm was the result of CH-4 in xylose nonreducing end unit.^{35,36} The assignment of chemical shifts for the bark alkaline extractives is summarized in Table 1.

Therefore, the liquid-state ¹³C NMR spectrum has confirmed that the bark alkaline extractives from mountain pine beetle-infested lodgepole pine contained tannin, degraded lignin, and degraded hemicellulose. The tannin and degraded lignin have molecular structures suitable for the phenolic resin synthesis.

Liquid-State ¹³C NMR Spectrum of the Liquefied Bark. The liquid-state ¹³C NMR spectrum of the phenol-liquefied bark is shown in Figure 2. The assignment of the chemical shifts was made based on previous publications.^{8–11} Multiple peaks within the ranges of 157–159, 129–131, 119–122, and 115–117 ppm were observed in the liquid-state ¹³C NMR spectrum of the

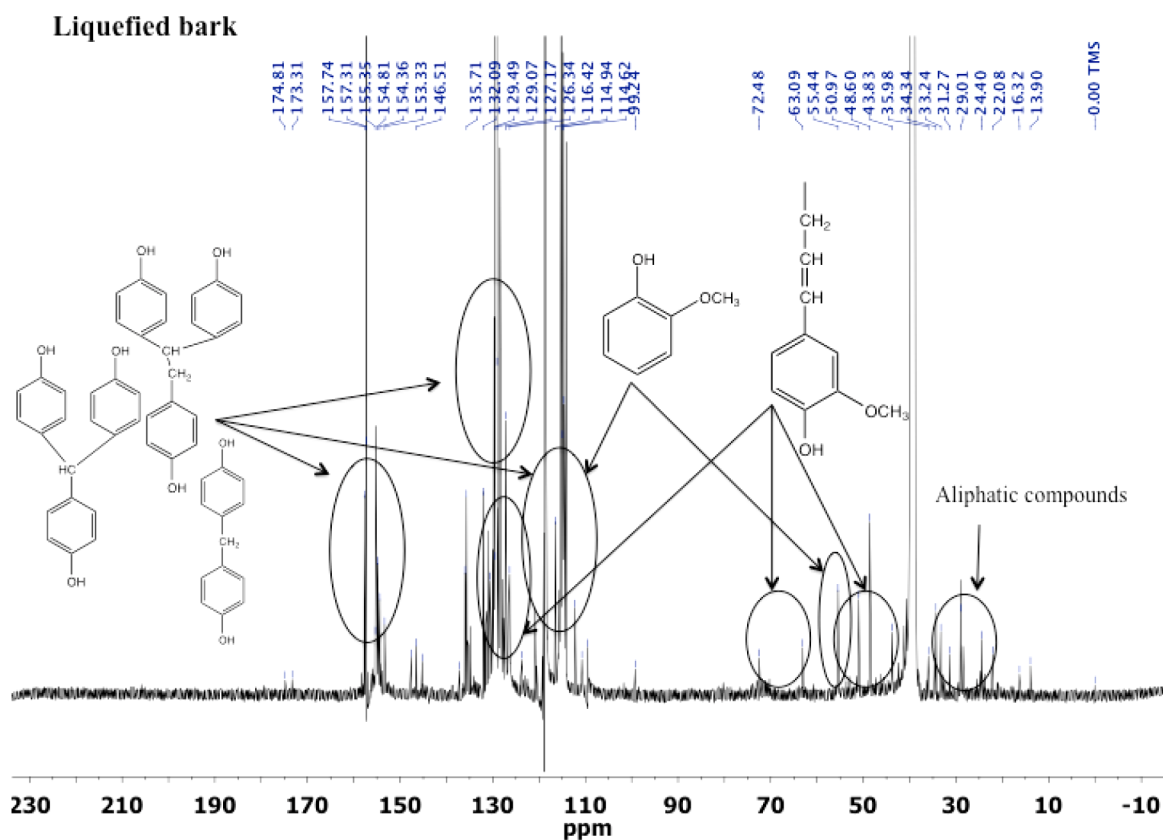


Figure 2. Liquid-state ^{13}C NMR spectrum of the liquefied bark.

liquefied bark. This indicated that there were both free phenol and phenolated bark components with combined phenol structures in the liquefied bark, because free phenol is expected to be represented by chemical shifts of C–OH at 158.5 ppm, *ortho*-carbon at 115.9 ppm, *meta*-carbon at 130.1 ppm, and *para*-carbon at 121.3 ppm. The chemical shift at 174.8 ppm arose from the C=O group of the glucuronic acid, indicating that it reacted with the lignin and formed the ester linkage. The chemical shifts representing the C- β in β -O-4' and C- γ in β -O-4' at 86.0 and 60.1 ppm, respectively, were not observed in the liquefied bark, implying that the β -aryl ether structure of lignin was split during the liquefaction. The chemical shift at 72.5 ppm was from C- α in β -O-4' (erythro) guaiacyl. The chemical shift at 55.5 ppm was the methoxyl groups (–OCH₃). Guaiacylglycerol- α -phenyl- β -guaiacyl structure in the liquefied bark was observed with C- γ at 63.1 ppm, guaiacyl unit from 110–130 ppm with C1 in etherified guaiacyl unit at 134.8 ppm, C4 in nonetherified guaiacyl unit at 145.3 ppm, and C4 in etherified guaiacyl unit in β -5'. The phenylcoumaranes, benzocyclobutanes, triphenylethanes, diphenylmethanes, and guaiacol structures and fragments were also observed in the liquefied bark, which were formed mainly by lignin during the phenol liquefaction reactions.

Phenylglucopyranoside, 2-glucopyranosylphenol, 4-glucopyranosylphenol, and 4-(2-hydroxyphenyl)-4-(4-hydroxyphenyl)-1,2,3-butanetriol derived from the cellulose liquefaction were observed in the liquefied bark. However, the intensity of the chemical shifts from 73 to 80 ppm representing the –CH–OH and –CH₂OH in the polysaccharide were very weak, suggesting that these compounds have been converted into tri(4-hydroxyphenyl)methane, 1,1,2-tri(4-hydroxyphenyl)ethane (strong chemical shifts at 150–160 and 120–130 ppm representing the phenolic structures in these products were

observed), and other phenolated products during the liquefaction. The assignment of chemical shifts for the liquefied bark is summarized in Table 2.

Table 2. Assignment of Chemical Shifts for Liquefied Bark^{8–11}

chemical shifts (ppm)	assignment
174.83	glucouronic acid
157–159	C–OH on the phenolic ring
146.51	C4 in etherified guaiacyl unit in β -5'
145.25	C4 in nonetherified guaiacyl unit
134–135	C1 in etherified guaiacyl and syringyl unit
129–131	<i>meta</i> -carbons on the phenolic ring
119–122	<i>para</i> -carbon on the phenolic ring
115–117	<i>ortho</i> -carbon on the phenolic ring
110–130	guaiacyl unit
86	C- β in β -O-4'
73–80	–CH–OH and –CH ₂ OH in the polysaccharide
72.5	C- α in β -O-4' (erythro) guaiacyl
63.1	C- γ in guaiacylglycerol- α -phenyl- β -guaiacyl structure
60.1	C- γ in β -O-4'
55.5	methoxyl groups

Overall, the process of bark liquefaction in phenol appeared to be similar to wood liquefaction in phenol. The bark components underwent degradation and chemical bond formation/cleavage during the liquefaction, followed by reactions of the degraded products with phenol to form phenolated components. Compared with bark alkaline extractives, more phenolic structures were found in the liquefied bark.

Liquid-State ^{13}C NMR Spectrum of the Lab-Made Phenol-Formaldehyde Resin. The liquid-state ^{13}C NMR

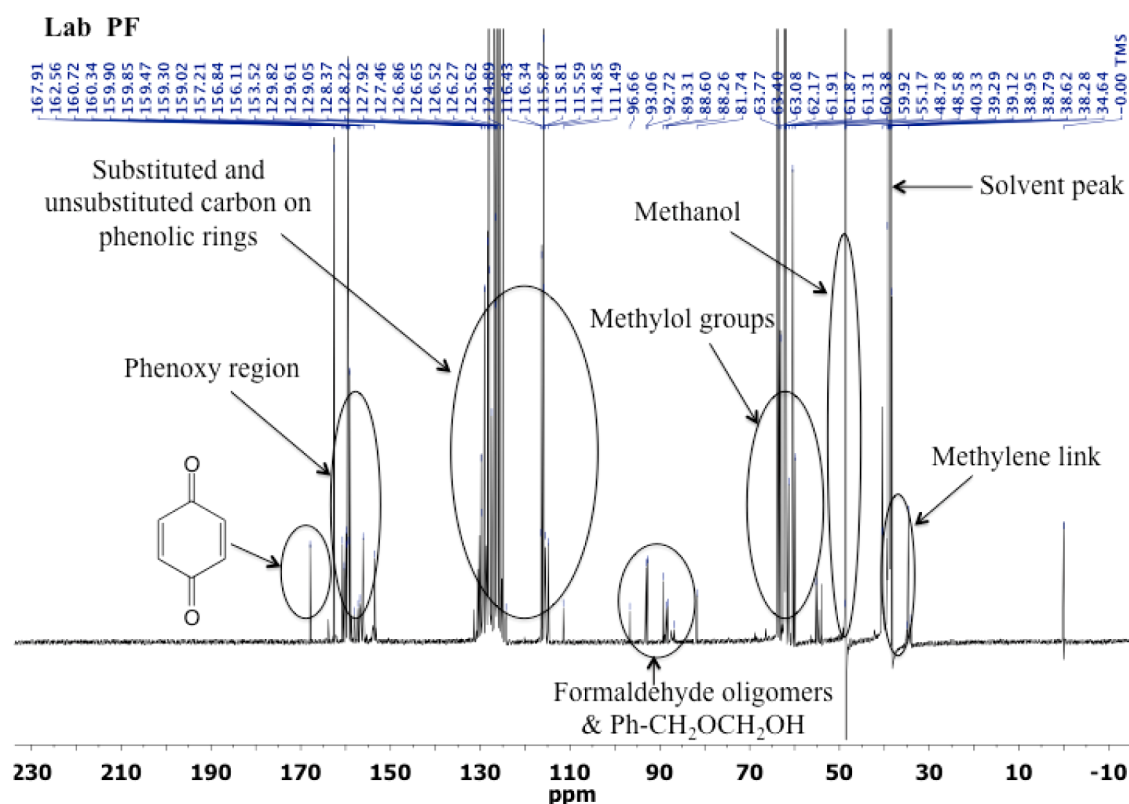


Figure 3. Liquid-state ^{13}C NMR spectrum of the lab PF resin.

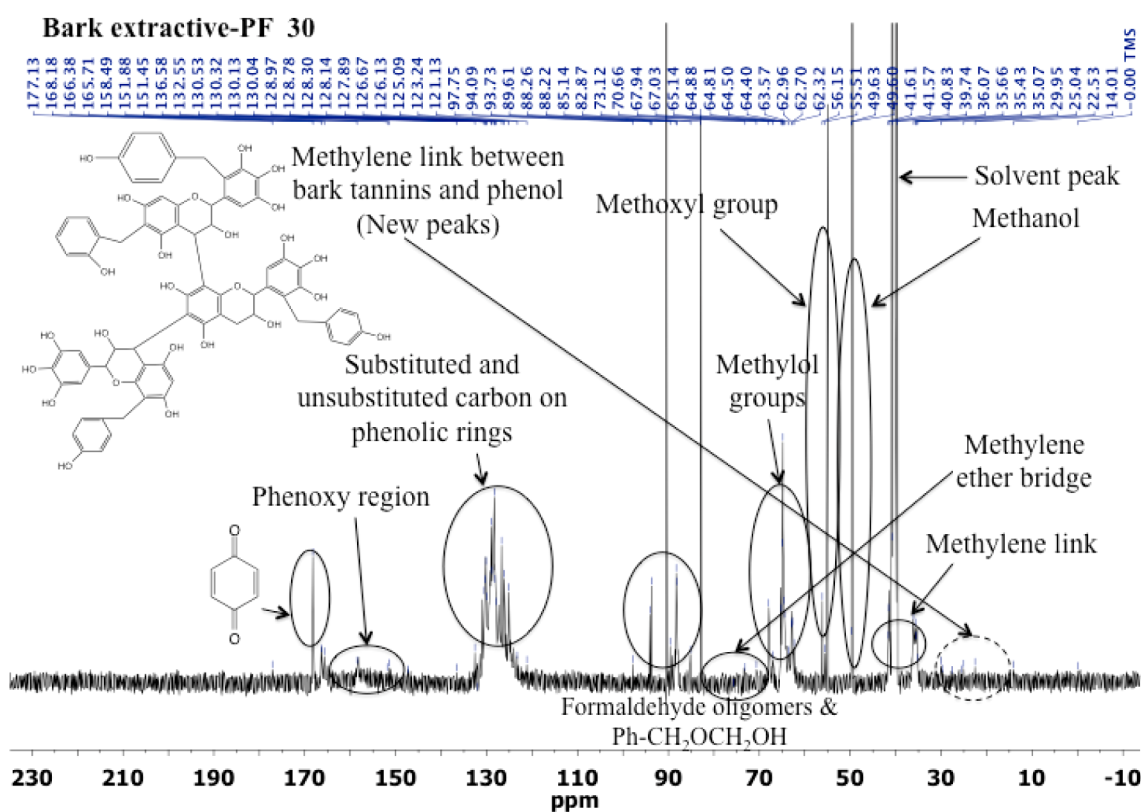


Figure 4. Liquid-state ^{13}C NMR spectrum of bark extractive-PF resin with 30 wt % phenol substitution by the bark extractives.

spectrum of the lab PF resin was shown in Figure 3. The chemical shifts were assigned to the corresponding functional groups based on previous findings.^{17,18,21,22}

The chemical shifts at 153.5–163.9 ppm were assigned to phenoxy carbons. The chemical shifts of *para*-alkylated phenolic groups were between 158.0 and 159.5 ppm, which showed higher

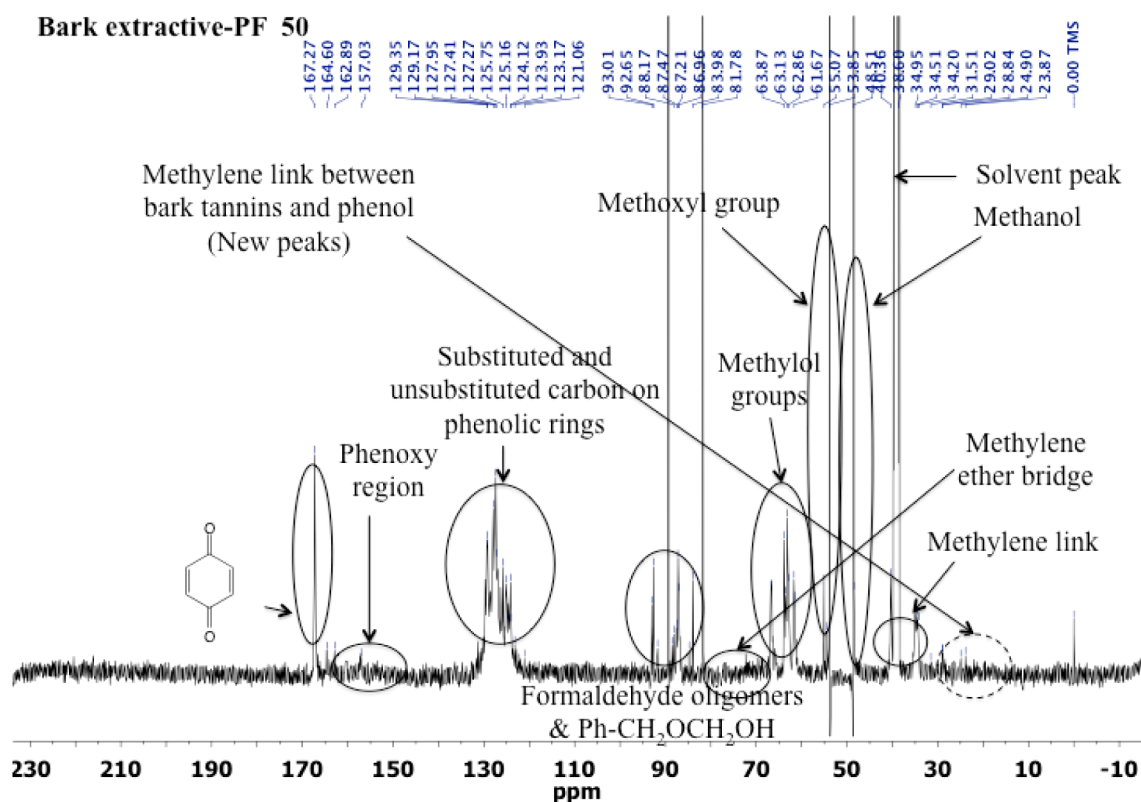


Figure 5. Liquid-state ¹³C NMR spectrum of bark extractive-PF resin with 50 wt % phenol substitution by the bark extractives.

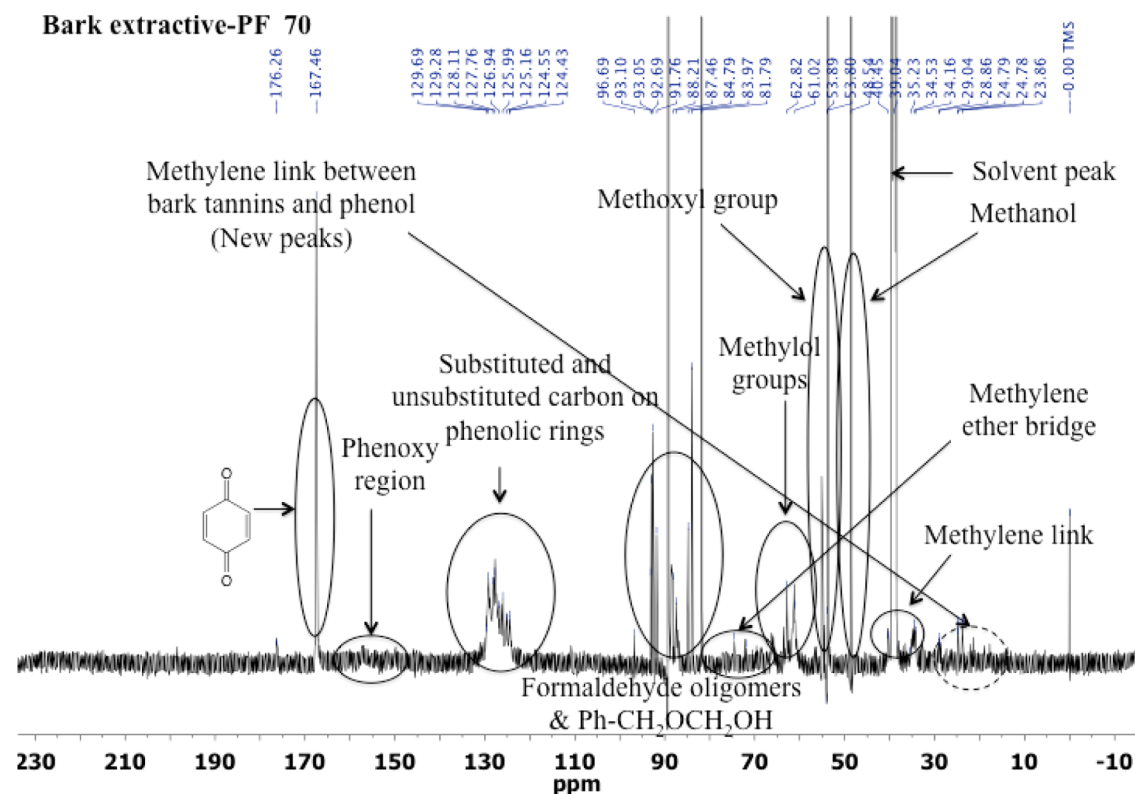


Figure 6. Liquid-state ¹³C NMR spectrum of bark extractive-PF resin with 70 wt % phenol substitution by the bark extractives.

intensities than those of chemical shifts of *ortho*-alkylated phenolic groups between 153.5 and 157.2 ppm. The chemical shifts of phenoxy carbons varied with the changes of pH of the resin due to the changes of polarity of the phenoxy groups.

The chemical shift at 48.7 ppm was due to methanol (CH₃OH). Methanol is commonly used in formaldehyde solution as a stabilizer. Methanol could also be formed during the resin synthesis from the Cannizzaro reaction of formaldehyde

under a strong alkaline condition. The chemical shift at 55.2 ppm was assigned to the methyl carbon in hemiformal ($\text{CH}_3\text{OCH}_2\text{OH}$), with the methylene carbon chemical shift at 89.3 ppm ($\text{CH}_2\text{OCH}_2\text{OH}$).

The chemical shift at 81.7 ppm was related to the unreacted formaldehyde in the PF resins. The small peaks around 86–87 ppm belonged to formaldehyde oligomers. The addition reaction products of *ortho*-hemiformal and *para*-hemiformal have the chemical shift at 89.3 ppm for the carbon connected to the hydroxyl ($\text{Ph}-\text{CH}_2\text{OCH}_2\text{OH}$) and at 63.1–63.7 ppm for the carbon connected to the phenolic ring ($\text{Ph}-\text{CH}_2\text{OCH}_2\text{OH}$). The chemical shifts at 92.1–93.7 ppm for the *ortho*- and *para*- $\text{Ph}-\text{CH}_2\text{OCH}_2\text{OCH}_2\text{OH}$ were also observed. No peaks were found between 69 and 73 ppm, indicating that the methylene ether bridges were not formed between the phenolic rings during the synthesis of the PF resins under the selected experimental conditions. This was consistent with previously published results.^{20,22,24,26} *Ortho*–*ortho* links of methylene groups between phenols at 29.2–29.6 ppm were not observed in the spectrum ($\text{Ph}-\text{CH}_2-\text{Ph}$), while the *ortho*–*para* and *para*–*para* links of methylene groups at 34.6–35.0 and 39.1 ppm were observed. It is understandable because the *ortho*–*ortho* methylene links are not favored in the presence of sodium hydroxide.^{21,22} The peaks at 114–116 ppm of unsubstituted *ortho* aromatic carbons of phenol and the peaks at 120–124 ppm of unsubstituted *para* aromatic carbons of phenol were observed. The peaks at 60.4–63.4 ppm represented the methylol groups ($\text{Ph}-\text{CH}_2\text{OH}$) in the PF resins, with the *ortho* link at 60.4–62.8 ppm and the *para* link at 63.1–63.4 ppm.

Liquid-State ^{13}C NMR Spectrum of Bark Extractive Phenol-Formaldehyde Resins. The differences in the liquid-state ^{13}C NMR spectra between the bark-extractive PF resin (Figure 4) and the lab PF resin (Figure 3) could be observed clearly. The incorporation of bark extractives in the formulation of the phenolic resins introduced new peaks (shown in Figures 4–6).

The appearance of the new chemical shifts at 29.3–30.9, 28.8–29.1, and 23.8–24.9 ppm in the bark extractive-PF resins could be attributed to the methylene groups between phenol and the tannin-B ring (29.3–30.9 ppm) and between phenol and the tannin-A ring (phloroglucinol ring, 28.8–29.1, 23.9–24.9 ppm),^{14,15,37,41} which were not observed in the lab PF. These new peaks provided evidence that the tannin components (both A ring and B ring) in the bark extractives reacted with formaldehyde during the resin synthesis. In general, tannin-A ring is more reactive than tannin-B ring toward formaldehyde; however, the reactivity of tannin-B ring could be increased when the pH of the reaction system is >10 .¹ The intensity of these peaks increased with the increasing amount of bark extractives in the resin synthesis.

Past studies reported that the phenolic compounds in the bark extractives could be used as accelerators for PF resins in particle board and plywood production because of their ability to minimize gelation and shorten press time.^{38–40} Previously published differential scanning calorimeter (DSC) results have found that the introduction of bark extractives to the PF resin synthesis affected the curing behavior and curing kinetics of the resulting bark extractive-PF resins.^{2,3} The bark extractive-PF resins showed faster curing rates than the lab PF resin did. The reactions between the tannin components in the bark alkaline extractives and formaldehyde could be one of the reasons for the acceleration of the curing rates of the bark extractives-PF resins.

The intensities of the chemical shifts at 60–65 and 35–37 ppm, which were attributed, respectively, to methylol groups and methylene groups adjacent to phenol rings, were weaker in the bark extractives-PF resins than in the lab PF resins. With the increasing level of phenol substitution by the bark extractives in the resin synthesis, the intensities of these chemical shifts in the bark extractives-PF resins decreased. This is likely due to the fact that, as more phenol was replaced by the bark extractives, less methylol groups and methylene groups can be formed between phenols. Meanwhile, the structures of the bark extractives could also introduce steric hindrance to the reactions between phenol and formaldehyde. A small chemical shift at 71–73 ppm, which indicated the existence of the methylene ether bridges, was observed in the spectrum of bark extractives-PF resins but not in the spectrum of the lab PF resin.

In the spectra of the bark extractive-PF resins with different levels of phenol substitution, the intensities of chemical shifts for the unsubstituted *para* carbons of phenol at 120–124 ppm were lower than those of the lab PF resin. The chemical shifts at 115–116 ppm, which correspond to the unsubstituted *ortho* aromatic carbons of phenol, were absent. This suggested that the *ortho* aromatic carbons of phenol had completely reacted after the introduction of bark extractives to the PF resin. Similar observations have been reported in the literature for the PF resin, and the reason was that the *ortho* substitution was more favored by the addition of curing accelerators.^{19,23,24} Therefore, bark alkaline extractives have the potential to speed up the resin curing reactions.

Methoxy groups as shown at 54.3 ppm were clearly observed in the bark extractive-PF resins, and the peak intensities increased with the increasing amount of bark extractives in the resin synthesis. The intensity of chemical shift at 89.3 ppm of the $\text{Ph}-\text{CH}_2\text{OCH}_2\text{OH}$ increased significantly in the bark extractive-PF resins.

The intensities of the chemical shifts at 150–160 ppm due to phenoxy groups decreased significantly in the spectra of bark extractive-PF resins when compared to the spectrum of the lab PF resin. These chemical shifts were almost invisible in the spectrum of bark extractive-PF resins with 70% phenol replacement. The chemical shifts at 166–168 ppm, which represent carbonyl groups in bark extractive-PF resin, increased in intensities with the increasing level of phenol substitution. The carbonyl groups in the lab PF resins were formed by the oxidation of the phenolic rings to quinone structures during and after the resin synthesis. The carbonyl groups in the bark extractive-PF resins may have originated from the bark extractives or the oxidation of the phenolic rings or both. The assignment of chemical shifts for the lab PF resin and bark extractive-PF resins is summarized in Table 3.

Table 4 shows the ratios of the relevant functional groups related to phenolic rings. In comparison with lab PF resin, the bark extractive-PF resins had a higher of *para*/*ortho* methylol ratio and a lower amount of *para*–*para*/*ortho*–*para* methylene bridges. For the lab PF resin, the substitution occurred more at the *para* positions than at the *ortho* positions and *para*-methylol groups reacted more easily with other *para* positions to form *para*–*para* links. When the amount of the free *para* positions decreased, the reaction with *ortho* positions increased and led to the decrease in the *para*/*ortho* ratio of methylol and the *para*–*para*/*ortho*–*para* methylene links. However, the bark extractives allowed the *ortho* position of phenol to react more favorably with formaldehyde than the *para* position, and the bark extractives also resulted in more *ortho*–*para* methylene linkage formation in

Table 3. Assignment of Chemical Shifts for the Lab PF Resin and Bark-Derived PF Resins^{14,15,17,18,25–27,37,41}

chemical shifts (ppm)	assignment
166–168	carbonyl C=O
153.5–163.9	phenoxy carbons
153.5–157.2	phenoxy, alkylated in ortho position
158.0–159.5	phenoxy, alkylated in para position
129.0–130.4	substituted para aromatic carbons of phenol
126.0–128.1	substituted ortho aromatic carbons of phenol
120.0–124.0	unsubstituted para aromatic carbons of phenol
114.0–116.6	unsubstituted ortho aromatic carbons of phenol
86–93.7	formaldehyde oligomers, Ph–CH ₂ OCH ₂ OH
81.7	unreacted formaldehyde in the resins
72.0–76.0	C- α in the β -O-4' guaiacyl unit
69.0–73.0	phenolic methylene ether bridges
63.1–64.7	<i>para</i> -methylol
60.4–62.8	<i>ortho</i> -methylol
54.3	methoxyl groups
48.7–50	methanol
39.1–41	<i>para</i> – <i>para</i> methylene linkage
34.6–35.0	<i>ortho</i> – <i>para</i> methylene linkage
29.3–29.6	<i>ortho</i> – <i>ortho</i> methylene linkage
29.3–30.9	methylene linkage on tannin-B ring
28.8–29.1, 23.9–24.9	methylene linkage on tannin-A ring

Table 4. Ratios of the Relevant Functional Groups Related to Phenolic Rings

sample	para/ortho (–CH ₂ OH)	p–p/o–p link (–CH ₂ –)	unsubstituted/ substituted hydrogen (–H/– CH ₂ OH)	methylol/ methylene– (CH ₂ OH/– CH ₂ –)
lab PF	0.18	1.97	0.18	3.76
bark extractive- PF 30	2.04	0.57	0.16	1.56
bark extractive- PF 50	0.98	0.82	0.14	1.44
bark extractive- PF 70	0.31	0.74	0.11	1.36
liquefied bark-PF	0.73	1.17	0.42	3.68

the bark extractive-PF resins than in the lab PF resin, which yielded a lower ratio of *para*–*para*/*ortho*–*para* methylene links in the bark extractive-PF resins.

The methylol/methylene ratio and the ratio of unsubstituted/substituted hydrogen (–H/–CH₂OH) of the bark-extractive PF resins were lower than those of the lab PF resin. These two ratios decreased with increasing level of phenol substitution by the bark extractives. The addition of bark extractives reduced the unsubstituted hydrogen and methylol/methylene ratio of the resulting bark extractive-PF resins; at this stage the resins were more reactive toward formaldehyde to form a further cross-link, which was consistent with the previously reported DSC results.^{2,3}

Liquid-State ¹³C NMR Spectrum of the Liquefied Bark-Phenol Formaldehyde Resin. The liquid-state ¹³C NMR spectrum of the liquefied bark-PF resin is shown in Figure 7. The intensities of the chemical shifts of the phenoxy groups at 150–160 ppm were similar to those of the bark extractive-PF resins, which were weaker than those of the lab PF resin. The chemical shifts at 164–167 ppm represent carbonyl groups of the liquefied

bark-PF resin. The methoxy group from the liquefied bark components was clearly observed at 55.5 ppm in the spectrum of the liquefied bark-PF resin. The chemical shifts at 71–76 ppm represent the C- α in the β -O-4' guaiacyl unit as well as the methylene ether bridges.

Compared with the bark extractive-PF resins, the intensities of the chemical shifts at 60–65 and 35–37 ppm attributed to methylol groups and methylene groups, respectively, were stronger in the liquefied bark-PF resin. It is reasonable to expect that the newly formed phenolated products are generally highly reactive and easily react with formaldehyde to form methylol groups. However, the intensities of the chemical shifts of methylol groups and methylene groups in the liquefied bark-PF resin were weaker than those of the lab PF resin, indicating that the liquefied bark had retarded the reaction of phenol with formaldehyde, probably due to steric hindrance resulting from the larger molecular structures. The chemical shifts at 120–130 ppm of the substituted and unsubstituted phenolic rings in the liquefied bark-PF resin had higher intensities than those of the bark extractive-PF resins, probably due to phenolation of the bark components.

Besides *para*–*para* and *ortho*–*para* methylene links at 34–35 and 40–41 ppm, respectively, the *ortho*–*ortho* methylene link with a lower intensity at 29.3 ppm was also observed for the liquefied bark-PF resin, which was absent from the bark extractive-PF resins and the lab PF resin. Another difference between the bark extractive-PF resins and the liquefied bark-PF resin was the presence of the chemical shifts at 115–116 ppm for the unsubstituted ortho carbons of phenol in the liquefied bark-PF resin. It could also be concluded that the phenolic rings attached to the degraded bark components during liquefaction were mostly located at their *para* positions. The major differences in the spectra of the bark extractive-PF resins, liquefied bark-PF resin, and lab PF resins are summarized in Table 5.

These differences in the molecular characteristics are likely due to the differences in the structures of the liquefied bark and bark extractives. Bark after phenolation likely possessed a large amount of new phenolic rings, such as tri(4-hydroxyphenyl)methane, 1,1,2-tri(4-hydroxyphenyl)ethane, etc., as shown in Figure 2. These products are highly reactive and can further condense with formaldehyde, phenol, or each other. During the condensation reaction with formaldehyde, *ortho*–*ortho* methylene links were formed. The liquefied bark could be considered as a curing accelerator for the liquefied bark-PF resin since it promoted the *ortho* substitution.^{23,24} Meanwhile, due to the steric hindrance of the phenolated products, the *ortho* position on the phenolic rings could not be easily accessed; as a result, unsubstituted *ortho* carbons of phenol were observed in the liquefied bark-PF resin.

The liquefied bark-PF resins had a higher *para*/*ortho* (–CH₂OH) methylol group substitution and a lower ratio of *para*–*para*/*ortho*–*para* methylene bridges than the lab PF resin did. It indicated that the liquefied bark also enhanced the formation of *ortho*–*para* methylene linkage in the liquefied bark-PF resin when compared to the lab PF resin. The liquefied bark-PF resins had a higher ratio of *para*–*para*/*ortho*–*para* methylene bridges than the bark extractive-PF resin did due to its higher steric hindrance effects, i.e., the *ortho* position of the phenolic rings was blocked or hard to access. The methylol/methylene ratio of the liquefied bark-PF resin was lower than that of the lab PF resin but higher than that of the bark extractive-PF resins, whereas the ratio of unsubstituted/substituted hydrogen (–H/–CH₂OH) of the liquefied bark-PF resin was higher than those of

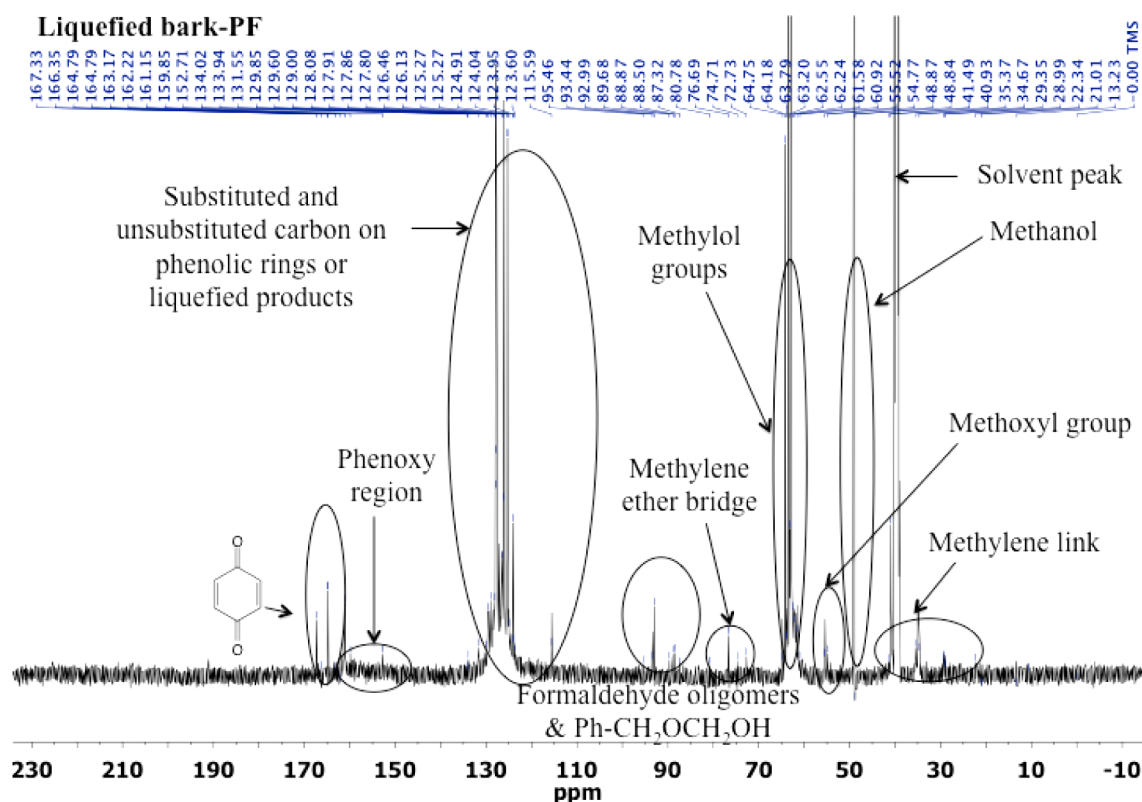


Figure 7. Liquid-state ^{13}C NMR spectrum of the liquefied bark-PF resin.

Table 5. Summary of the Major Spectral Differences of the Resins

resins	major differences based on liquid-state ^{13}C NMR spectra
lab PF	unsubstituted ortho and para aromatic carbons of phenol were observed; no methylene ether linkage; no ortho-ortho methylene linkage
bark extractive-PF	methylene ether linkage, methoxy group, methylene linkage between phenol and tannins, unsubstituted para carbons of phenol were observed; no unsubstituted ortho aromatic carbons of phenol and no ortho-ortho methylene linkage
liquefied bark-PF	methylene ether linkage, guaiacyl units, methoxy group, ortho-ortho methylene linkage, unsubstituted ortho and para carbons of phenol were observed

the lab PF and bark extractive-PF resins. This also supported the hypothesis that the liquefied bark had more reactive sites toward formaldehyde than the bark extractives did, but the steric hindrance of its structures might have slowed down the addition and condensation reactions.

Relationship between the Resin Molecular Structures and Curing Performance.

Previous differential scanning

calorimeter (DSC) measurement results showed that the bark-derived PF resins had faster curing rates than the lab PF resin.^{2,3} The curing activation energies for the lab PF resin, liquefied bark-PF resin, bark extractive-PF with 30 wt % phenol substitution level, bark extractive-PF resin with 50 wt % phenol substitution level, and bark extractive-PF with 70 wt % phenol substitution level were 70.22, 78.12, 79.98, 79.40, and 83.38 kJ/mol, respectively. The pre-exponential factors, which indicate the curing rates for the lab PF resin, liquefied bark-PF resin, bark extractive-PF with 30 wt % phenol substitution level, bark extractive-PF resin with 50 wt % phenol substitution level, and bark extractive-PF with 70 wt % phenol substitution level were 1.59×10^8 , 2.98×10^9 , 2.78×10^9 , 2.73×10^9 , and $7.55 \times 10^9 \text{ s}^{-1}$, respectively. Combining these past findings from DSC measurements with the liquid-state ^{13}C NMR results in this study, it can be seen that the inclusion of bark components in phenolic resin synthesis, either in the form of phenol liquefied bark or in the form of bark alkaline extractives, affects the molecular structures and curing behavior of the resulting resins.

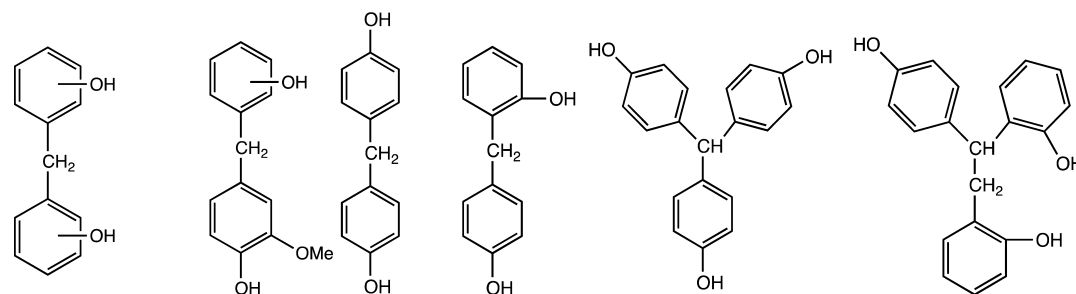


Figure 8. Possible liquefied products from acid-catalyzed phenol liquefaction of bark.

In comparison with the lab PF resin, the faster curing rates indicated by the pre-exponential factor of the bark extractive-PF resins were most likely due to the tannin compounds in the bark extractives. The phloroglucinol structure of tannin-A rings had a higher reactivity toward formaldehyde than phenol did. It accelerated the curing rates of the phenolic resins.^{38–40} Furthermore, the addition of bark extractives to the resin synthesis seemed to facilitate the ortho substitution of phenol instead of the para substitution. It also promoted more formation of para–ortho methylene link than para–para methylene link and reduced the unsubstituted hydrogen. All these factors could have contributed to the faster curing rates of the resulting bark extractive-PF resins.

For the liquefied bark-PF resin, phenolated products (Figure 8) of degraded lignin (diphenylmethanes and guaiacol) and degraded cellulose (methylolphenols) as well as other fragments with newly generated multiphenolic rings in the structures were more reactive toward formaldehyde and could help the resin cure faster. The phenolated bark in the resin synthesis favored the formation of ortho–ortho methylene linkage. The phenolated bark also made the formation of an ortho–para methylene link more favorable than a para–para methylene link. The higher ratio of para–para/ortho–para methylene bridges, higher methylol/methylene ratio, and higher ratio of unsubstituted/substituted hydrogen ($-H/-CH_2OH$) of the liquefied bark-PF resin indicated the existing steric hindrance effect of the liquefied bark, which could retard the curing reactions.

Additionally, the larger molecules of the liquefied bark and bark extractives with lower molecular mobility could make it difficult for the resulting resins to form cross-links;^{8–11,33} therefore, the curing activation energies of the bark-derived PF resins were higher than that of the lab PF resin. However, the reactive sites on the liquefied bark or bark extractives still had the potential to accelerate the curing process of resins at higher temperatures. The self-condensation reactions of the liquefied bark components and bark extractives could also contribute to the relatively high pre-exponential factors and faster curing rates of the bark-derived PF resins despite having higher curing activation energies.

CONCLUSIONS

The introduction of bark components to the phenol formaldehyde resin synthesis affected the resins structures and curing characteristics. Bark-derived PF resins exhibited higher curing activation energies but higher curing pre-exponential factors than the lab PF resin. Methylene ether bridges were observed in the bark-derived PF resins. Bark components were incorporated into the resulting resin structures as reactants.

Tannin structures of mainly procyanidin type, consisting of phloroglucinol A-ring, catechol B-ring, and pyrogallol B-ring, were observed in the alkaline extractives of mountain pine beetle-infested lodgepole pine bark. Lignin and hemicellulose fragments were also observed in the bark alkaline extractives. The tannin components in the bark alkaline extractives reacted with formaldehyde during the phenolic resin synthesis and accelerated the curing rate of the resulting resins. The addition of bark alkaline extractives to the phenolic resin synthesis made the ortho substitution of phenol more favorable than the para substitution. The bark extractive-PF resins had a higher para/ortho methylol group substitution, a lower ratio of para–para/ortho–para methylene bridges, and a lower ratio of unsubstituted/substituted hydrogen ($-H/-CH_2OH$) than the lab PF resin.

Phenolated products of degraded lignin and degraded cellulose, such as triphenylethanes, diphenylmethanes, and guaiacol and fragments with new phenolic rings in the structures, were observed in the phenol-liquefied bark. The phenolic rings attached to the degraded bark components during liquefaction were mostly at the para position. The phenolated products can accelerate the curing rate of the liquefied bark-PF resin. Ortho–ortho methylene bridges and unsubstituted ortho position of the phenolic rings were observed in the liquefied bark-PF resin. The liquefied bark-PF resins had a higher ratio of para/ortho ($-CH_2OH$) methylol group substitution, a higher ratio of unsubstituted/substituted hydrogen ($-H/-CH_2OH$), and a lower ratio of para–para/ortho–para methylene bridges than the lab PF resin. The liquefied bark-PF resins had a higher ratio of para–para/ortho–para methylene bridges, a higher methylol/methylene ratio, and a higher ratio of unsubstituted/substituted hydrogen ($-H/-CH_2OH$) than bark extractive-PF resin. Phenol-liquefied bark had more reactive sites toward formaldehyde than bark alkaline extractives, but the steric hindrance could have retarded the addition and condensation reactions.

AUTHOR INFORMATION

Corresponding Author

*Tel.: +14169468070. Fax: +14169783834. E-mail: ning.yan@utoronto.ca.

Notes

The authors declare no competing financial interest.

ACKNOWLEDGMENTS

Dr. Tim Burrow of the NMR center, Department of Chemistry, University of Toronto, is highly appreciated for his help on the NMR measurements. Financial support from partners of Ontario Research Fund-Research Excellence project: Bark Biorefinery is highly acknowledged.

REFERENCES

- (1) Pizzi, A. *Wood Adhesives Chemistry and Technology*; Marcel Dekker Inc.: New York, 1993; Vol. 1, pp 177–246.
- (2) Zhao, Y.; Yan, N.; Feng, M. Characterization of phenol-formaldehyde resins derived from liquefied lodgepole pine barks. *Int. J. Adhes. Adhes.* **2010**, *30*, 689–695.
- (3) Zhao, Y.; Yan, N.; Feng, M. Bark extractives-based phenol-formaldehyde resins from beetle-infested lodgepole pine. *J. Adhes. Sci. Technol.* **2012**, DOI: 10.1080/01694243.2012.697689.
- (4) Yazaki, Y.; Collins, P. J. Wood adhesives from *Pinus radiata* bark. *Holz Roh-Werkst* **1994**, *52*, 185–190.
- (5) Yazaki, Y.; Collins, P. J. Wood adhesives based on tannin extracts from barks of some pine and spruce species. *Holz Roh-Werkst.* **1994**, *52*, 307–310.
- (6) Jenkin, D. J. Adhesives from *Pinus radiata* bark extractives. *J. Adhes.* **1984**, *16*, 299–310.
- (7) Stefani, P. M.; Peña, C.; Ruseckaite, R. A.; Piter, J. C.; Mondragon, I. Processing conditions analysis of *Eucalyptus globulus* plywood bonded with resol-tannin adhesives. *Bioresour. Technol.* **2008**, *99*, 5977–5980.
- (8) Lin, L. Z.; Yao, Y. G.; Yoshioka, M.; Shiraishi, N. Liquefaction mechanism of cellulose in the presence of phenol under acid catalysis. *Carbohydr. Polym.* **2004**, *57*, 123–129.
- (9) Lin, L. Z.; Yao, Y. G.; Shiraishi, N. Liquefaction mechanism of β -O-4 lignin model compound in the presence of phenol under acid catalysis. Part 1. Identification of the reaction products. *Holzforschung* **2001**, *55*, 617–624.
- (10) Lin, L. Z.; Nakagame, S.; Yao, Y. G.; Yoshioka, M.; Shiraishi, N. Liquefaction mechanism of β -O-4 lignin model compound in the presence of phenol under acid catalysis. Part 2. Reaction behavior and pathways. *Holzforschung* **2001**, *55*, 625–630.

- (11) Zhang, Y. C.; Ikeda, A.; Hori, N.; Takemura, A.; Ono, H.; Yamada, T. Characterization of liquefied product from cellulose with phenol in the presence of sulfuric acid. *Bioresour. Technol.* **2006**, *97*, 313–321.
- (12) Navarrete, P.; Pizzi, A.; Pasch, H.; Rode, K.; Delmotte, L. MALDI-TOF and ^{13}C NMR characterization of maritime pine industrial tannin extract. *Ind. Crops Prod.* **2010**, *32*, 105–110.
- (13) Thompson, D.; Pizzi, A. Simple ^{13}C NMR methods for quantitative determinations of polyflavonoid tannin characteristics. *J. Appl. Polym. Sci.* **1995**, *55*, 107–212.
- (14) Pizzi, A.; Stephanou, A. A comparative ^{13}C NMR study of polyflavonoid tannin extracts for phenolic polycondensates. *J. Appl. Polym. Sci.* **1993**, *50*, 2105–2113.
- (15) Pizzi, A.; Stephanou, A. A ^{13}C NMR study of polyflavonoid tannin adhesive intermediates. II. Colloidal state reactions. *J. Appl. Polym. Sci.* **1994**, *51*, 2125–2130.
- (16) Grigsby, W. J.; Hill, S. J.; McIntosh, C. D. NMR estimation of extractables from bark: Analysis method for quantifying tannin extraction from bark. *J. Wood Chem. Technol.* **2003**, *23*, 179–195.
- (17) Werstler, D. D. Quantitative ^{13}C NMR characterization of aqueous formaldehyde resins. I. Phenol-formaldehyde resins. *Polymer* **1986**, *27*, 750–756.
- (18) Kim, M. G.; Amos, L. W.; Barnes, E. Study of the reaction rates and structures of a phenol-formaldehyde resol resin by carbon-13 NMR and gel permeation chromatography. *Ind. Eng. Chem. Res.* **1990**, *29*, 2032–2037.
- (19) Park, B. D.; Riedl, B. ^{13}C NMR study on cure-accelerated phenol-formaldehyde resins with carbonates. *J. Appl. Polym. Sci.* **2000**, *77*, 841–851.
- (20) He, G. B.; Yan, N. ^{13}C NMR study on structure, composition and curing behavior of phenol-urea-formaldehyde resole resins. *Polymer* **2004**, *45*, 6813–6822.
- (21) Smit, R.; Pizzi, A.; Schutte, C. J.; Paul, S. O. The structure of some phenol-formaldehyde condensates for wood adhesives. *J. Macromol. Sci., Part A: Pure Appl. Chem.* **1989**, *26*, 825–841.
- (22) Grenier-Loustalot, M.; Larroque, S.; Grande, D.; Grenier, P.; Bedel, D. Phenolic resins: Influence of catalyst type on reaction mechanisms and kinetics. *Polymer* **1996**, *37*, 1363–1369.
- (23) Lei, H.; Pizzi, A.; Despres, A.; Pasch, H.; Du, G. B. Ester acceleration mechanisms in phenol-formaldehyde resin adhesives. *J. Appl. Polym. Sci.* **2001**, *100*, 3075–3093.
- (24) Luukko, P.; Alvila, L.; Holopainen, T.; Rainio, J.; Pakkanen, T. T. Effect of alkalinity on the structure of phenol-formaldehyde resol resins. *J. Appl. Polym. Sci.* **2001**, *82*, 258–262.
- (25) Fan, D. B.; Chang, J. M.; Li, J.; Mao, A.; Zhang, L. T. ^{13}C NMR study on the structure of phenol-urea-formaldehyde resins prepared by methylolureas and phenol. *J. Appl. Polym. Sci.* **2009**, *112*, 2195–2202.
- (26) Fan, D. B.; Chang, J. M.; Li, J. Z. On the structure and cure acceleration of phenol-urea-formaldehyde resins with different catalysts. *Eur. Polym. J.* **2009**, *45*, 2849–2857.
- (27) Vázquez, G.; López-Suevos, F.; Villar-Garea, A.; González-Alvarez, J.; Antorrena, G. ^{13}C NMR analysis of phenol-urea-formaldehyde prepolymers and phenol-urea-formaldehyde-tannin adhesives. *J. Adhes. Sci. Technol.* **2004**, *18*, 1529–1543.
- (28) Chuang, I. S.; Maciel, G. E. ^{13}C NMR investigation of the stability of a resol-type phenol-formaldehyde resin toward formalin, toward base, and toward nonoxidizing or oxidizing acid. *Macromolecules* **1991**, *24*, 1025–1032.
- (29) Lei, Y.; Wu, Q.; Lian, K. Cure kinetics of aqueous phenol-formaldehyde resins used for oriented strandboard manufacturing: analytical technique. *J. Appl. Polym. Sci.* **2006**, *100*, 1642–1650.
- (30) Lei, Y.; Wu, Q. Cure kinetics of aqueous phenol-formaldehyde resins used for oriented strandboard manufacturing: Effects of wood flour. *J. Appl. Polym. Sci.* **2006**, *102*, 3774–3781.
- (31) He, G. B.; Riedl, R.; Ait-Kadi, A. Model-free kinetics: Curing behavior of phenol formaldehyde resins by differential scanning calorimetry. *J. Appl. Polym. Sci.* **2003**, *87*, 433–440.
- (32) Pizzi, A.; Merlin, M. A new class of tannin adhesives for exterior particleboard. *Int. J. Adhes. Adhes.* **1981**, *1*, 261–264.
- (33) Pizzi, A. Phenolic and tannin-based adhesive resins by reactions of coordinated metal ligands. II. Tannin adhesive preparation, characteristics, and application. *J. Appl. Polym. Sci.* **1979**, *24*, 1257–1268.
- (34) Lorenz, K.; Preston, C. M. Characterization of high-tannin fractions from humus by ^{13}C cross-polarization and magic angle spinning nuclear magnetic resonance. *J. Environ. Qual.* **2002**, *31*, 431–436.
- (35) Sun, X. F.; Sun, R. C.; Fowler, P.; Baird, M. S. Extraction and characterization of original lignin and hemicelluloses from wheat straw. *J. Agric. Food Chem.* **2005**, *53*, 860–870.
- (36) Vázquez, G.; Antorrena, G.; González, J. ^1H and ^{13}C NMR characterization of acetosolv-solubilized Pine and Eucalyptus lignins. *Holzforschung* **1997**, *51*, 158–166.
- (37) Werstler, D. D. Quantitative ^{13}C NMR characterization of aqueous formaldehyde resins. 2. Resorcinol-formaldehyde resins. *Polymer* **1986**, *27*, 757–762.
- (38) Vázquez, G.; González-Alvarez, J.; Antorrena, G. Curing of a phenol-formaldehyde-tannin adhesive in the presence of wood. *J. Therm. Anal. Calorim.* **2006**, *84*, 651–654.
- (39) Chen, C. M. Copolymer resins of bark and agricultural residue extracts with phenol and formaldehyde: 40% weight of phenol replacement. *For. Prod. J.* **1982**, *32*, 14–18.
- (40) Fechtal, M.; Riedl, B. Use of eucalyptus and acacia mollissima bark extract-formaldehyde adhesives in particleboard manufacture. *Holzforschung* **1993**, *47*, 349–357.
- (41) Pizzi, A.; Horak, R. M.; Ferreira, D.; Roux, D. G. Condensates of phenol, resorcinol, phloroglucinol and pyrogallol as model compounds of flavonoid A- and B-rings with formaldehyde. *J. Appl. Polym. Sci.* **1979**, *24*, 1571–1578.